Fatigue Crack Initiation and Growth from an Induced Angled Crack Under Biaxial Bending - Part I

By
S. Y. Zamrik, A. Seibi, D. C. Davis

Department of Engineering Science and Mechanics
The Pennsylvania State University
University Park, Pa., USA, 16802

Third International Conference on
Biaxial/Multiaxial Fatigue
April 3-6, 1989 Stuttgart, FRG

ABSTRACT

Fatigue crack initiation and growth from induced surface flaws in a remotely-applied biaxial bending stress field was investigated. Semielliptical surface flaws were induced in rhombic plate specimens at angles oriented at different degrees with respect to the principal tensile stress direction. The plate specimens were simply supported and cycled by applying two bending moments using the anticlastic bending method.

Test results showed that crack grows in a direction of a fracture initiation angle θ_o under the influence of a hoop stress which is maximum at the crack tip and then grows in a direction and rate which dependent on the orientation of the induced surface flaw. Under biaxial bending, crack growth rates were found to increase as the initial flaw orientation approached a direction normal to the maximum principal stress. A model is proposed for dealing with crack initiation angle θ_o due to biaxial bending. The fracture surface, as a result of fatigue cycling, showed a mixed fracture behavior which was dependent on the applied biaxial stress ratio and induced crack angle β. The experimental results showed a trend similar to the proposed model but with some discrepancies.

INTRODUCTION

In the past two decades, most of the studies on mixed mode fatigue crack initiation and propagation problem were restricted to uniaxial loading despite the fact that in most cases, structures are subjected to complex loading system resulting in fatigue failure due to multi-or biaxial stress field. The mixed mode cracking is an interaction between Mode I and Mode II which can be simulated by rotating a known surface flaw at different angles with respect to a principal stress axis. Fracture criteria applied to this type of problem assumes that the initial fracture angle, θ_o as shown in Figure 1, can in general be determined from the stress field near the crack tip. Since a number of studies were conducted on mixed mode cracking under uniaxial loading, they can be considered as a special case of biaxial loading (biaxial stress ratio,

$\alpha = 0$). Among the first studies on this subject, the work of Erdogan and Sih [1] can be considered as the initial concern for mixed mode cracking. They treated the problem of a plate under uniform tension σ with an angled central crack of length 2a to determine the crack direction. They assumed that the crack grows in a direction θ_0 for which the hoop stress, σ_θ, at the crack tip is maximum. A few years later, Williams and Ewing [2] modified this theory by including the non-singular terms in the series expansion for better correlation. Later, Finnie and Saith [3] pointed out that the proposed modification neglected the contribution of the normal stress to the crack.

Among the models that were proposed to deal with mixed mode cracking, Swedlow's Model [4] was considered as a basic model for the biaxial stress investigation. Swedlow proposed a compression model to account for the crack closing and frictional effect in cracks under compression. He used Williams analysis [5] to derive general expressions for the stress distribution near the crack tip. These expressions are :

$$\sigma_r = \frac{K_I}{\sqrt{2\pi r}}\left[\frac{5}{4}\cos\frac{\theta}{2} - \frac{1}{4}\cos 3\frac{\theta}{2}\right]$$

$$+ \frac{K_{II}}{\sqrt{2\pi r}}\left[-\frac{5}{4}\sin\frac{\theta}{2} + \frac{3}{4}\sin 3\frac{\theta}{2}\right] + \sigma_t \cos^2\theta$$

$$\sigma_\theta = \frac{K_I}{\sqrt{2\pi r}}\left[\frac{3}{4}\cos\frac{\theta}{2} + \frac{1}{4}\cos 3\frac{\theta}{2}\right]$$

$$- \frac{3K_{II}}{4\sqrt{2\pi r}}\left[\sin\frac{\theta}{2} + \sin 3\frac{\theta}{2}\right] + \sigma_t \sin^2\theta$$

$$\tau_{r\theta} = \frac{K_I}{4\sqrt{2\pi r}}\left[\sin\frac{\theta}{2} + \sin 3\frac{\theta}{2}\right]$$

$$+ \frac{K_{II}}{\sqrt{2\pi r}}\left[\frac{1}{4}\cos\frac{\theta}{2} + \frac{3}{4}\cos 3\frac{\theta}{2}\right] - \sigma_t \sin\theta\cos\theta \qquad (1)$$

where:

$$K_I = \bar{\sigma}\sqrt{\pi a}\,(\sin^2\beta)$$
$$K_{II} = \bar{\sigma}\sqrt{\pi a}\,(\sin\beta\cos\beta)$$
$$\sigma_t = \bar{\sigma}(\cos^2\beta - \sin^2\beta) \qquad (2)$$

where a is the semi-elliptical crack length and $\bar{\sigma}$ is the applied stress .

To take into account the crack closing and the frictional effect, he suggested that $\bar{\sigma}$ should not be replaced by $-\bar{\sigma}$ to express a compressive model. He postulated that when K_I has negative values, it means that the crack is closing on itself and by such action, it causes friction on the surface of the crack. Thus, in compression, K_I can be neglected and Equations (1-3) can be expressed as:

$$\sigma_r = \frac{K_{II}}{\sqrt{(2\pi r)}}\left[-\frac{5}{4}\sin\frac{\theta}{2} + \frac{3}{4}\sin 3\frac{\theta}{2}\right]$$

$$+ \bar{\sigma}\left(\sin^2\theta - \mu_f \sin 2\theta\right)\sin^2\beta + \sigma_t \cos^2\theta$$

$$\sigma_\theta = \frac{3K_{II}}{4\sqrt{(2\pi r)}}\left[\sin\frac{\theta}{2} + \sin 3\frac{\theta}{2}\right]$$

$$+ \bar{\sigma}\left(\cos^2\theta - \mu_f \sin 2\theta\right)\sin^2\beta + \sigma_t \sin^2\theta$$

$$\tau_{r\theta} = \frac{K_{II}}{\sqrt{(2\pi r)}}\left[\frac{1}{4}\cos\frac{\theta}{2} + \frac{3}{4}\cos\frac{\theta}{2}\right]$$

$$+ \bar{\sigma}\left(\cos\theta\sin\theta - \mu_f \cos 2\theta\right)\sin^2\beta + \sigma_t \sin\theta\cos\theta \qquad (3)$$

where $\bar{\sigma} = -1$, μ_f is the coefficient of friction, and

$$K_{II} = \bar{\sigma}\sqrt{\pi\alpha}(\sin\beta\cos\beta - \mu_f \sin^2\beta) \qquad (4)$$

and

$$\sigma_t = \bar{\sigma}(\cos^2\beta - \sin^2\beta) \qquad (5)$$

Equations (3-5) are applicable along the crack faces. The coefficient of friction may take a static or dynamic value depending on the motion of the crack faces. Using the maximum hoop stress criterion of Erdogan and Sih and taking into account the crack closing and the friction effect, Swedlow was able through his model to predict the initial fracture angle, θ_o, for an inclined crack under uniaxial compression.

Another model related to this problem, is one proposed by Woo and Ling (6). They reviewed a number of fracture criteria dealing with angled crack initiation θ_o and its relation to crack inclination angle β. They examined the biaxial loading effect on the parameter used in each criterion for the prediction of the fracture behavior under mixed mode. In their experimental work, they used cruciform type specimens of 1/8 in. thickness with an initial crack length of 1-1/4 in. The material used in their investigation was polymethyl-methacrylate (PMMA). Their analysis was an extention of Swedlow's approach to the case of biaxial tension-compression stressed models. This was accomplished by modifying Swedlow's near-tip stress equations to the following forms:

$$\sigma_r = \frac{K_I}{\sqrt{(2\pi r)}}\left[\frac{5}{4}\cos\frac{\theta}{2} - \frac{1}{4}\cos 3\frac{\theta}{2}\right]$$

$$+ \frac{K_{II}}{\sqrt{(2\pi r)}}\left[-\frac{5}{4}\sin\frac{\theta}{2} + \frac{3}{4}\sin 3\frac{\theta}{2}\right] + \sigma_t \cos^2\theta$$

$$+ \sigma_n \sin^2\theta + \sigma_f \sin 2\theta$$

$$\sigma_\theta = \frac{K_I}{\sqrt{(2\pi r)}}\left[\frac{3}{4}\cos\frac{\theta}{2} + \frac{1}{4}\cos 3\frac{\theta}{2}\right]$$

$$- \frac{3K_{II}}{4\sqrt{(2\pi r)}}\left[\sin\frac{\theta}{2} + \sin 3\frac{\theta}{2}\right] + \sigma_t \sin^2\theta$$

$$+ \sigma_n \cos^2\theta - \sigma_f \sin 2\theta$$

$$\tau_{r\theta} = \frac{K_I}{4\sqrt{(2\pi r)}}\left[\sin\frac{\theta}{2} + \sin 3\frac{\theta}{2}\right]$$

$$+ \frac{K_{II}}{\sqrt{(2\pi r)}}\left[\frac{1}{4}\cos\frac{\theta}{2} + \frac{3}{4}\cos 3\frac{\theta}{2}\right] - \sigma_t \sin\theta\cos\theta$$

$$+ \sigma_n \sin\theta\cos\theta + \sigma_f \cos 2\theta \qquad (6)$$

where

σ_n = normal compression stress on the crack faces
σ_f = frictional resistance due to the compressive stress ($=\mu_f \sigma_n$)
μ_f = friction coefficient
$\sigma_t = \sigma(1-\alpha)\cos 2\beta$

They stated that the terms in the above equations will not appear at the same time and the selection of the proper terms for a given problem was listed in a tabulated form as shown in Table (1). On the basis of their experimental work, they concluded that the maximum hoop stress criterion was the most appropriate one to use for both the open and closed crack conditions.

Analysis of Crack Initiation Angle vs Induced Angled Crack

On the basis of cited approaches, a biaxial stress model to predict crack initiation angle, θ_o, with respect to an inclined crack angle β is presented. The basis of the near-tip stress problem

solution can be derived from Williams' analysis which was given in the form of series expansion. The hoop stress expression, σ_θ, shown in Figure 2, was expressed as:

$$\sigma_\theta = \sqrt{\frac{a}{2r}} \cos\frac{\theta}{2}\left(\sigma_{y'}\cos^2\frac{\theta}{2} - \frac{3\tau_{x'y'}}{2}\sin\theta \right) + \sigma_{x'}\sin^2\theta + \sqrt{\frac{2r}{a}} F(\sigma_{y'}, \tau_{x'y'}, \theta) + \dots \quad (7)$$

where $\sigma_{x'}$, $\sigma_{y'}$ and $\tau_{x'y'}$ represent, respectively, the parallel stress, the normal stress and the shear stress applied at the crack surface as shown in Figure 3. The angled induced surface flaw is also shown in terms of β, θ_o, and stress biaxiality ratio α. It should be noted that the first term in equation (7) produces a singularity as r approaches 0, where r and a express the variation of both $\sigma_{x'}$ and $\tau_{x'y'}$ due to the presence of the crack. The second term represents the stress parallel to the crack and is simply superimposed on the stress distribution; hence, it is not affected by r and a. For a localized region near the crack tip, only the first term is considered since it dominates the solution.

Using the maximum hoop stress criterion, postulated by Erdogan and Sih, the initial crack angle, θ_o, can be obtained if the following conditions are satisfied:

$$\sigma_\theta\Big|_{\theta_o} > 0, \quad \left[\frac{\partial\sigma_\theta}{\partial\theta}\right]_{\theta o} = 0 \quad , \quad \left[\frac{\partial^2\sigma_\theta}{\partial\theta^2}\right]_{\theta o} < 0 \quad (8)$$

by setting $\lambda = \sqrt{2r/a}$ and using the conditions in equation (8), the direction of the initial crack growth angle can be obtained by maximizing equation (7) and setting $\partial\sigma\theta / \partial\theta = 0$ resulting in:

$$\sigma_{y'} - \left[\frac{1-3\cos\theta}{\sin\theta}\right]\tau_{x'y'} - \frac{16\lambda}{3}\left[\frac{\sin\frac{\theta}{2}}{\tan\theta}\right]\sigma_{x'} = 0 \quad (9)$$

Equation (9) is the general expression for maximizing the hoop stress which can be solved for the initial crack angle for a given stress field. The expressions for $\sigma_{x'}$, $\sigma_{y'}$ and $\tau_{x'y'}$ depends on the nature of the loading condition (uniaxial or biaxial). Both Williams and Ewing, and Finnie and Saith used the above equation to predict the initial fracture angle for an inclined crack under uniaxial loading.

The stress equations used by Williams and Ewing were expressed as:

$$\sigma_{x'} = \sigma\cos^2\beta$$

$$\sigma_{y'} = \sigma\sin^2\beta$$

$$\tau_{x'y'} = \sigma\sin\beta\cos\beta \qquad (10)$$

whereas the equations used by Finnie and Saith were expressed as:

$$\sigma_{x'} = \sigma(\cos^2\beta - \sin^2\beta)$$

$$\sigma_{y'} = \sigma\sin^2\beta$$

$$\tau_{x'y'} = \sigma\sin\beta\cos\beta \qquad (11)$$

Note that the only difference between them is the expression of $\sigma_{x'}$.

Both methods have been extended to biaxial loading. This extension is based on equations (9,10,11) where the initial fracture angle for an inclined induced surface flaw under biaxial loading was determined using the conditions in equation (8).

In order to determine the stresses applied to a crack of length 2a (Figure 3), a prismatic element is considered as shown in Figure 4 where the three faces are respectively perpendicular to the x, y, and y'. The areas ΔA, $\Delta A\sin\beta$, and $\Delta A\cos\beta$ represent respectively the oblique, horizontal and vertical faces. The forces exerted on theses faces are also shown. Using the components along x' and y' axes, the equilibrium force equations are:

$$\sum F_{y'} = 0: \quad \sigma_{y'}\Delta A - \alpha\sigma(\Delta A\cos\beta)\cos\beta - \sigma(\Delta A\sin\beta)\sin\beta = 0 \qquad (12)$$

and

$$\sum F_{x'} = 0: \quad \tau_{x'y'}\Delta A + \alpha\sigma(\Delta A\cos\beta)\sin\beta - \sigma(\Delta A\sin\beta)\cos\beta = 0 \qquad (13)$$

Solving the first equation for $\sigma_{y'}$ and the second for $\tau_{x'y'}$, we obtain:

$$\sigma_{y'} = \sigma(\sin^2\beta + \alpha\cos^2\beta) \qquad (14)$$

$$\tau_{x'y'} = (1-\alpha)\sigma\sin\beta\cos\beta \qquad (15)$$

Note that $\sigma_{y'}$ and $\tau_{x'y'}$ are equivalent to Mode I and Mode II stress intensity factors K_I and K_{II}.

The expression for the stress, $\sigma_{x'}$, parallel to the crack surface, can be obtained from equation (14) by replacing β by $\beta+90^o$, which is the angle formed between the x axis and the x' axis. To better understand the presence of the parallel stress to the crack, a Mohr's circle approach is

constructed as shown in Figure 5 which shows the stresses along the x-y and the x'-y' planes. Note that the stresses applied at the prismatic element, and as shown in Figure 4 are principal stresses. Therefore, it was necessary to rotate this element by an angle β , in order to determine the stresses applied at the crack surface, $\sigma_{x'}$, $\sigma_{y'}$ and $\tau_{x'y'}$. The angle β is the orientation angle of the induced surface flaw with respect to the maximum tensile stress. Therefore, equation (14) becomes:

$$\sigma_{x'} = \sigma[\sin^2(\beta + 90) + \alpha\cos^2(\beta + 90) \tag{16}$$

Using the following trigonometric identities:

$$\cos^2\theta = \frac{1+\cos 2\theta}{2}, \quad \sin^2\theta = \frac{1-\cos 2\theta}{2} \tag{17}$$

Equation (16) becomes:

$$\sigma_{x'} = \frac{\sigma}{2}[(1-\cos 2\beta) + \alpha(1+\cos 2\beta)] \tag{18}$$

and equation (18) reduces to:

$$\sigma_{x'} = \sigma[\cos^2\beta + \frac{\alpha}{2}(1-\cos 2\beta)] \tag{19}$$

or

$$\sigma_{x'} = \sigma(\cos^2\beta + \alpha\sin^2\beta) \tag{20}$$

By substituting the values of $\sigma_{x'}$, $\sigma_{y'}$ and $\tau_{x'y'}$ from equations (14,15,20) into equation (9), we have:

$$(\alpha + \tan^2\beta) - (1-\alpha)\left[\frac{1-3\cos\theta}{\sin\theta}\right]\tan\beta$$

$$-\frac{16\lambda}{3}\left[\frac{\sin\frac{\theta}{2}}{\tan\theta}\right](1+\alpha\tan^2\beta) = 0 \tag{21}$$

Equation (21) is the proposed model for relating θ to β and α in a biaxial stress state. The roots of equation (21) are denoted by θ_0. We can reduce equation (21) to the uniaxial case by letting $\alpha = 0$, which will then take the form of:

$$\tan^2\beta - \left[\frac{1-3\cos\theta}{\sin\theta}\right]\tan\beta - \frac{16\lambda}{3}\left[\frac{\sin\frac{\theta}{2}}{\tan\theta}\right] = 0 \tag{22}$$

Note that equation (22) is similar to Williams and Ewing equation for uniaxial loading and which was given as:

$$\tan^2\beta - \frac{1-3\cos\theta}{\sin\theta}\tan\beta - \frac{16\lambda}{3}\frac{\sin\frac{\theta}{2}}{\tan\theta} = 0$$

The solution of equation (21) is presented in Figure 6 showing the initial fracture angle, θ_o, as a function of the induced crack angle, β, for values of biaxiality ratios, α, ranging between -1.0 and 0. Note that, for small values of crack angles, β, at a given biaxiality ratio, α, a wide deviation is observed giving high values of θ_o. The reason for this deviation is the effect of σ_y' . For example, for $\beta = 45^o$ and $\alpha = -1.0$, $\sigma_y' = 0$; for $\beta \leq 45^o$, σ_y' becomes negative causing a closing effect rather than an opening effect on the crack surface. Therefore, there are two cases to be considered; (1) the opening mode as expressed by equation (21) where σ_y' is positive, and (2) the closing mode where σ_y' is negative. To account for the closing effect σ_y' should be eliminated from equation (21); otherwise, the solution of equation (9) is invalid. Therefore, setting $\sigma_y' = 0$, equation (21) becomes:

$$(1-\alpha)\left[\frac{1-3\cos\theta}{\sin\theta}\right]\tan\beta - \frac{16\lambda}{3}\left[\frac{\sin\frac{\theta}{2}}{\tan\theta}\right](1+\alpha\tan^2\beta) = 0 \qquad (23)$$

Hence, modification of equation (21) as expressed by (23) shifts the curve downward for better correlations of experimental data as shown in Figure 7. Note that both curves deviate from one another for $\beta \leq 45^o$ and merge together starting from $\beta = 45^o$ to $\beta = 90^o$ due to σ_y' effect. The solid curve represents the theoretical results of equation (21) where σ_y' was included; whereas, the dashed curve represents results without σ_y'. A comparison of the proposed model as expressed by equation (23) to Woo and Ling approach, is shown in Figure 8. It can be seen that both curves are in close agreement.

Experimental Procedure:

An experimental procedure which relates fatigue crack initiation and growth rates of surface flaw subjected to biaxial stress field was developed by Zamrik et al (7). The test method utilizes anticlastic bending of plates which produces a two-dimensional stress field. The anticlastic bending causes one surface of the plate curvature to be in compression while the other one in tension. Thus, the two generated curvatures see pure bending moments, M_{xx} and M_{yy} as shown in Figure 9. This type of loading produces negative values of biaxiality ratios $\alpha = \sigma 2 / \sigma 1$. In this study, ratios of α = -0.45, and -1.0 were used. Detailed description of the apparatus can be found in Zamrik's publications (8-9). For this program, the goal was aimed at generating biaxial data which could be used for: (1) determining the initial fracture angle, θ_o, at both tips of an induced surface flaw of given geometry, (2) compute the crack growth rate as the surface crack grows from the initial crack, and (3) establish a good understanding of fracture surface flaws subjected to mixed mode loading.

By setting a constant load amplitude, fatigue tests were conducted at two cycles per seconds (2 Hz). The material used in this study was 6061-T651 aluminum alloy plate specimens with nominal thickness of 0.25 inches. The material had a yield stress of 40.9 ksi (0.2% offset) and an ultimate tensile strength of 44.5 ksi with a tensile elongation of 13.6%. A semielliptical surface flaw with a geometry of 0.03 to 0.04 inches deep by 0.125 in. long by 0.005 in. wide was induced into the plate specimen by means of an electro-discharge machining (EDM) process. The orientation of the induced surface flaw, with respect to the principal tensile stress direction, was designated by the angle β. Prior to testing, the surface of each specimen was polished to a luster with different grades of metallurgical abrasive papers. Polishing wheels were also used to refine the surface around the EDM flaw so that a propagating crack could be readily observed under light microscope. The finished plate specimens are known as rhombic plate specimens.

Test Results and Discussion:

The test results of the research program dealing with crack initiation and propagation rate under biaxial bending are divided into three parts. Part I, which is the subject of this paper, deals only with fatigue crack initiation angle of mixed mode under biaxial loading. Part II deals with the prediction of crack trajectory as compared to the actual crack path for a number of biaxiality ratio with different inclined crack angles β. Part III deals with fatigue crack growth rate for rhombic plates as function of cyclic life to failure using the strain energy density factor and cyclic stress intensity factor approaches.

Two different geometries of rhombic plates were used producing biaxiality ratios of α = -0.45 with initial crack angle β of 30, 45, and 60 degrees and α= -1.0 with β = 0, 45, 60, 75, and 90 degrees. The loading conditions were kept the same during testing where the maximum applied load, P_{max}, was held at 850 lb. producing a maximum tensile stress of σ = 20,400 psi. The choice of P_{max} had to satisfy two conditions: (1) the stress intensity factor must be greater than the threshold stress intensity factor, and (2) P_{max} must be below the yield load, P_y, which was equal to 1040 lb. The initial fracture angles, θ_{oA} and θ_{oB}, shown in Figure 10, were measured optically by using a 40x projection microscope with a movable platform. The image of the crack usually showed a band with an upper and lower edge giving different values of 0_o within two degrees. Also, two measurements of fracture angles were taken, one at a small distance from the crack tip and the other one almost twice the distance of the first one. The plot of the experimental data with respect to the theoretical models is shown in Figures 11 and 12 in terms of fracture angle θ_0 vs induced crack angle β. Published approaches of Sih and Woo and Ling are also imposed. It is evident from the plots that discrepancy exists between the models and experimental data. The discrepancy can be attributed to a number of observations: (1) the fact that the models consider only two dimensional stress problems achieved by using thin specimens; (2) whereas, in this investigation the rhombic plate specimens are thick with respect to other investigators' specimens; (3) it is suspected, based on observed failure modes,

that a three dimensional state of stress exists in the rhombic plate specimens; (4) another factor contributing to the discrepancy could be related to the exclusion of higher terms in the series expansion of the stress and displacement equations. However, in predicting the crack trajectory (to be published as part II), the trajectory model is in agreement with the experimental data as shown in Figure 13.

It was also observed that when the induced crack angle β is between 45 and 90 degrees, the crack is in an opening mode due to the fact that the tensile stress is normal to the crack surface, and when β is greater than 0 but less than 45 degrees, the normal stress on the crack becomes compressive causing a crack closure.

Conclusions:

From the data obtained on thick plate specimens, it is concluded that within the experimental accuracy, the proposed model based on Woo and Ling (modified Swedlow's model) is limited to thin plate specimens subjected to a two-dimensional stress state. Once the state of stress is changed to a three dimensional problem, the models cannot predict accurately the crack initiation angle under mixed mode loading. However, the results have shown a consistent pattern similar to the model prediction. The discrepancy can be attributed to the use of thick plate specimens where the state of stress is three dimensional which seems to influence the crack initiation angle, but not the crack propagation rate and crack trajectory which fall under the influence of a biaxial state of stress once the crack has moved away from the initiation stages. Another factor in the discrepancy could be in selecting the size of the flaw 1.25 in. vs. 0.125 in. The overall observation, which can be stated in a positive way, is that the proposed models are not too far off from the thick plate experimental data and with further analysis, the initial fracture angle can be well predicted.

REFERENCES:

1. Erdogan, F. and Sih, G. C., "On the crack extension in plates under plane loading and transverse shear," J. Basic Engng., Vol. 85, 1963, pp.519-525.

2. Williams, J. G. and Ewing, P. D., "Fracture under complex stress," Int. J. Fracture Mech., Vol.8, 1972, pp.441-446.

3. Finnie, I. and Saith, A., "A note on the angled problem and directional stability of crack," Int. J. Fracture Mech., Vol.9, 1973, pp. 484-486.

4. Swedlow, J. L., "Criterion for growth of the angled crack," Cracks and Fracture, ASTM STP 601, 1976, pp.506-521.

5. Williams, J. G., "On the stress distribution at the base of a stationary crack," J. App. Mech., Vol. 24, 1957, pp.109-114.

6. Woo, C. W. and Ling, L. H.,"On angled crack initiation under biaxial loading," J. of Strain Analysis, Vol. 19, No.1, 1984, pp.51-59.

7. Zamrik, S. Y. and Goto, T., "The use of octahedral shear strain theory in biaxial low cycle fatigue," Materials Technology-An Interamerican Approach, ASME Conference on Materials Technology, 1968, pp.551-562.

8. Shabara, M. A., and Zamrik, S. Y., " Fatigue crack growth rate under conditions of a biaxial stress field'" Ph.D. Thesis, The Pennsylvania State University, 1976.

9. Zamrik, S. Y. and Allison, D. E., "The effect of surface flaw orientation on fatigue crack growth due to biaxial bending," ASME, Design Technology, DE-Vol.9, 1987, pp.81-86.

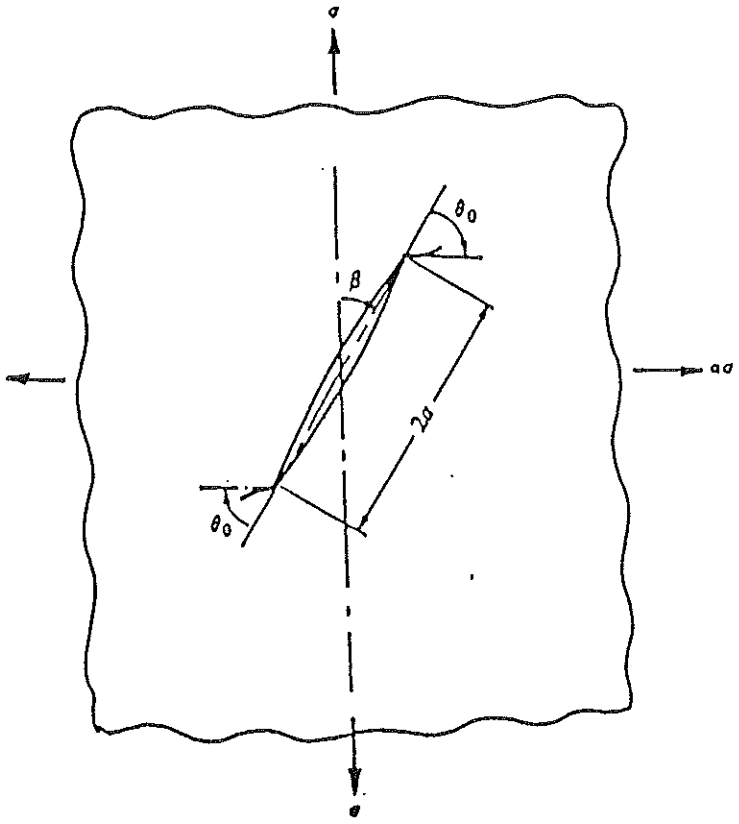

Figure 1. Angled Crack Under Biaxial Loading

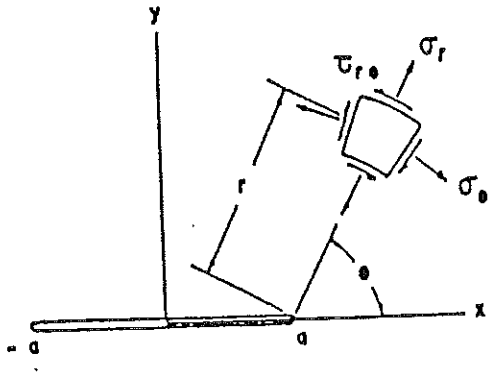

Figure 2. Stress Components Near the Crack Tip in Cylindrical Coordinates

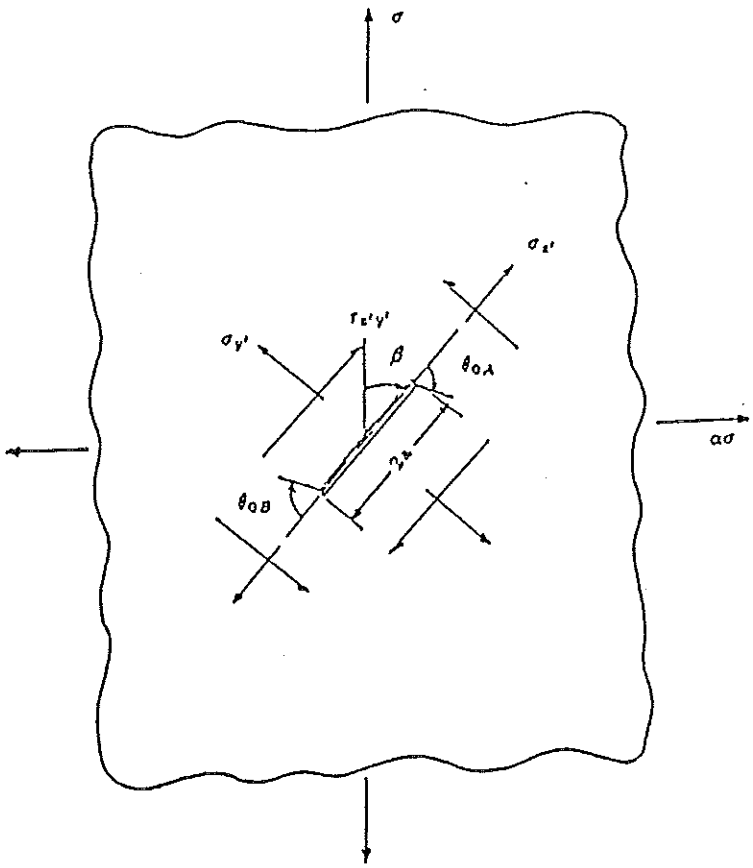

Figure 3. Angled Crack Representation

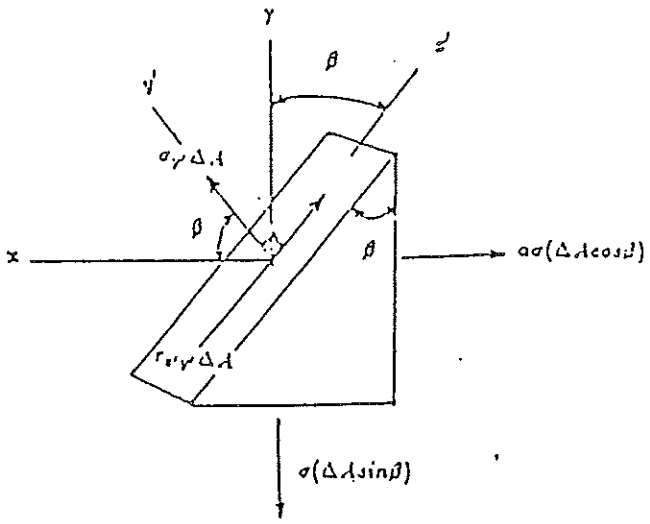

Applied Forces

Figure 4. Crack Element

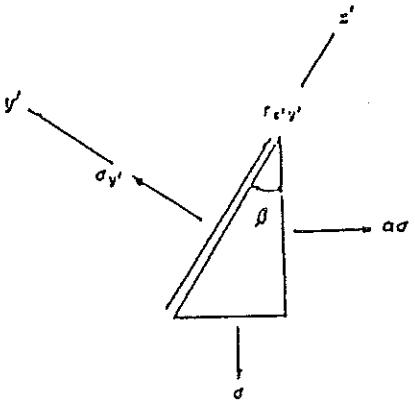

(a) Applied Forces

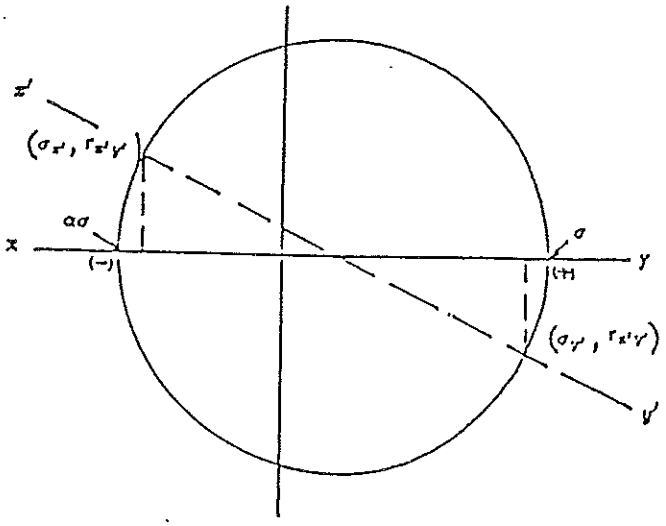

(b) Mohr's Circle

Figure 5. Crack Element and Mohr's Circle Configurations

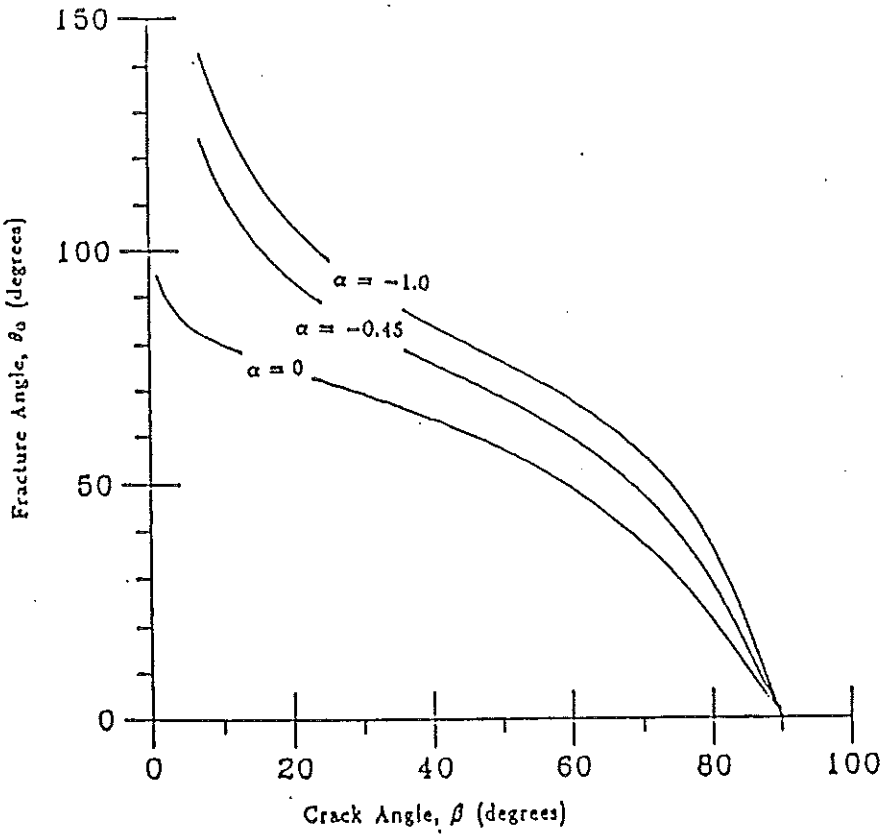

Figure 6. Fracture Angle, θ_0, Versus Crack Angle, β

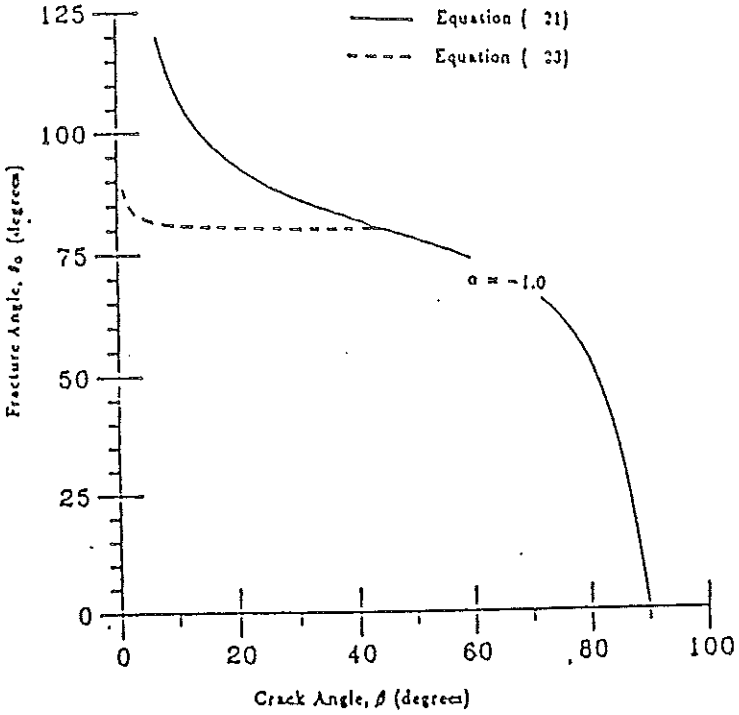

Figure 7. $\theta_0 - \beta$ Relationship for Biaxiality Ratio, $\alpha = -1.0$

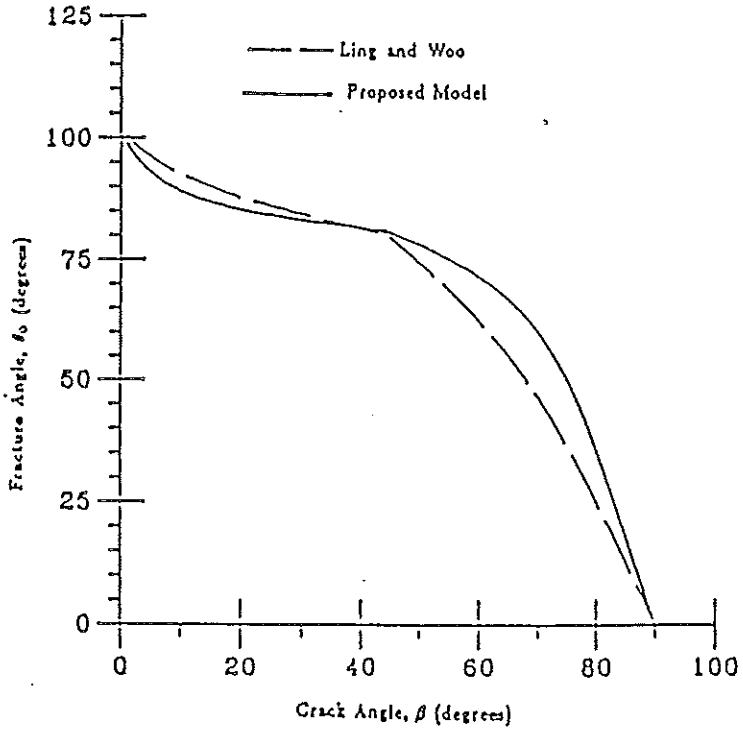

Figure 8. Comparison between the Proposed Method and Ling and Woo Method for $\alpha = -1.0$

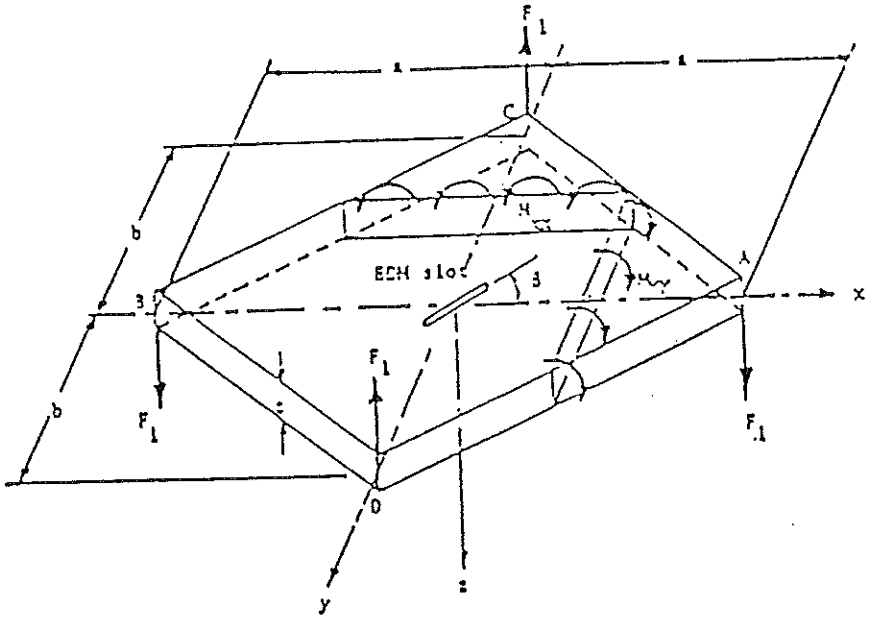

Figure 9 . Anticlastic Bending of Rhombic Plate

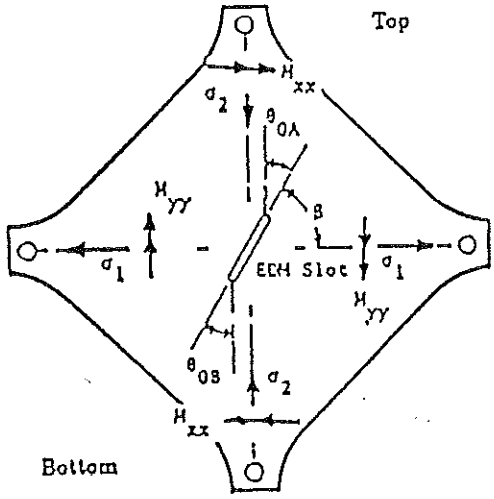

Figure 10. Anticlastic Plate Specimen With EDM Slot and Various Crack Angles

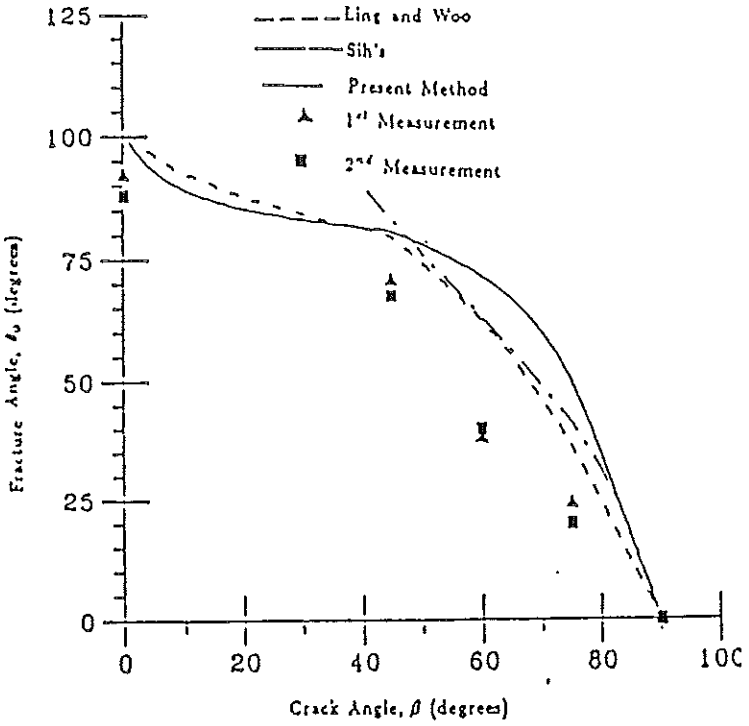

Figure 11. $\theta_0 - \beta$ Relationship for Biaxiality Ratio, $\alpha = -1.0$

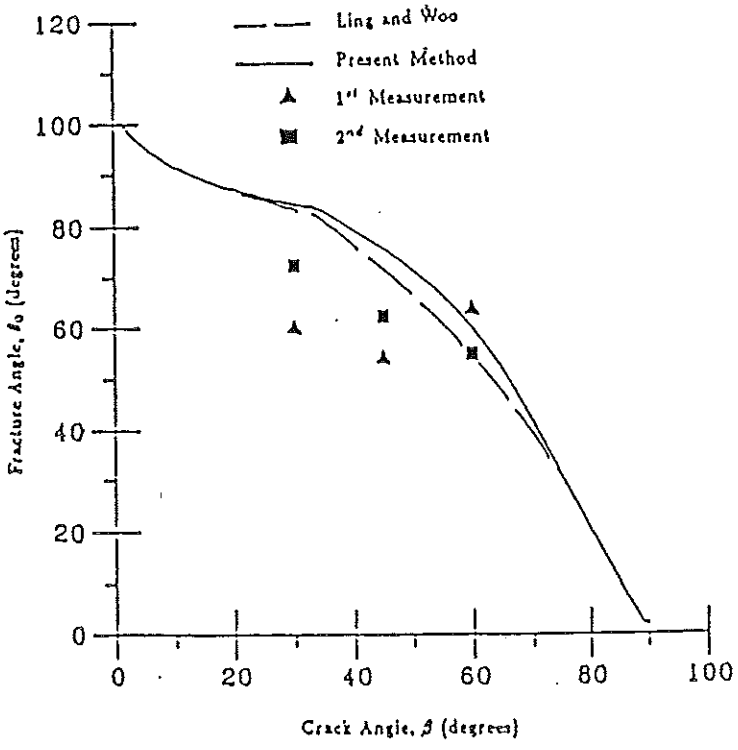

Figure 12. $\theta_0 - \beta$ Relationship for Biaxiality Ratio, $\alpha = -0.45$

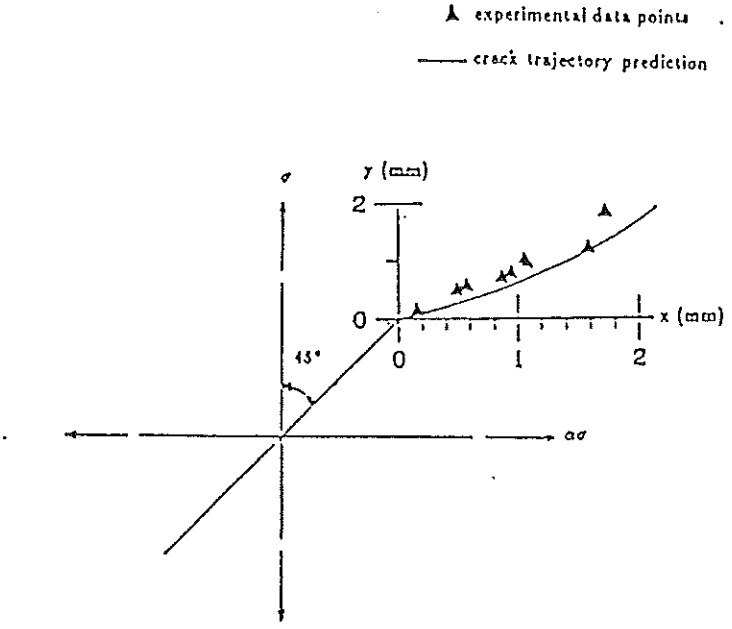

Figure 13. Mixed Mode Fatigue Crack Trajectory for an Inclined Surface Flaw With $\beta = 45°$ and $\Delta\sigma = 20{,}400$ psi

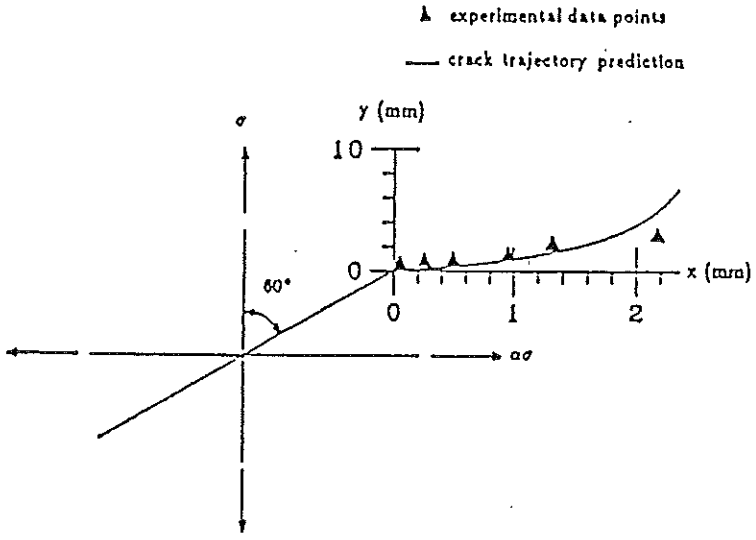

Figure 14. Mixed Mode Fatigue Crack Trajectory for an Inclined Surface Flaw With $\beta = 60°$ and $\Delta\sigma = 20{,}400$ psi

Table .1. List of The Conditions For Choosing The Proper Terms.

Ling and Woo

Loading conditions \ Selection of terms	K_I	K_{II}	σ_1	σ_2	σ_t
$\alpha > 0$	$\sigma\sqrt{(\pi a)}(\sin^2\beta + \alpha\cos^2\beta)$	$\sigma\sqrt{(\pi a)}(1-\alpha)\sin\beta\cos\beta$	$\sigma(1-\alpha)\cos 2\beta$		
$\alpha < 0$; $\sigma\sin^2\beta > \lvert\alpha\rvert\sigma\cos^2\beta$	$\sigma\sqrt{(\pi a)}(\sin^2\beta + \alpha\cos^2\beta)$	$\sigma\sqrt{(\pi a)}(1-\alpha)\sin\beta\cos\beta$	$\sigma(1-\alpha)\cos 2\beta$		
$\alpha < 0$; $\lvert\alpha\rvert\sigma\cos^2\beta \geq \sigma\sin^2\beta$; $\sigma\sin\beta\cos\beta(1-\alpha) > \mu\sigma(\lvert\alpha\rvert\cos^2\beta - \sin^2\beta)$		$\sigma\sqrt{(\pi a)}\{(1-\alpha)\sin\beta\cos\beta + \mu\sigma(\alpha\cos^2\beta + \sin^2\beta)\}$	$\sigma(1-\alpha)\cos 2\beta$	$\sigma(\alpha\cos^2\beta + \sin^2\beta)$	
Ditto (in Swedlow's form)		$\sigma\sqrt{(\pi a)}\{(1-\alpha)\sin\beta\cos\beta + \mu\sigma(\alpha\cos^2\beta + \sin^2\beta)\}$	$\sigma(1-\alpha)\cos 2\beta$	$\sigma(\alpha\cos^2\beta + \sin^2\beta)$	$\mu\sigma(\alpha\cos^2\beta + \sin^2\beta)$